Green, Vol. **1** (2011), pp. 65–80  DOI 10.1515/GREEN.2011.009

Review

# Intermediate Layers in Tandem Organic Solar Cells

**Yongbo Yuan,**[1] **Jinsong Huang**[1,*] **and Gang Li**[2]

[1] Department of Mechanical Engineering, University of Nebraska-Lincoln, Lincoln, NE 68588

[2] Solarmer Energy, Inc., El Monte, CA 91731

**Abstract.** Tandem structures can boost the efficiency of organic solar cell to more than 15%, compared to the 10% limit of single layer bulk heterojunction devices. Design and fabricating of intermediate layers plays a very important role to achieve high device performance. This article will review the main experimental progresses of tandem organic solar cells, and focus on the intermediate layers (charge recombination layers) in both thermal evaporated and solution processed organic tandem solar cell devices.

**Keywords.** Organic solar cell, tandem structure, intermediate layer.

**PACS®(2010).** 78.56.-a, 73.90.+f, 78.67.Pt.

## 1 Introduction

Industrialization and human development of the world have increased the demands for renewable energy. Renewable energy has been widely viewed as the grand challenge of the new century. In 2008, the world's energy consumption was 15 Terawatt (TW) per year [1], which is 20 times more than it was in 1850. 80% to 90% of the energy consumption per year was from the combustion of fossil fuels like coal and oil, which leave a heavy environmental footprint. Among all the energy sources, solar energy represents the most abundant and promising solution. The solar radiation on the Earth per hour is ∼14 TW, i.e. almost the same as the world's annual energy consumption. In fact, using photovoltaic (PV) modules with 10% efficiency, the total U.S. energy demand could be met by a 100 mile × 100 mile PV array in Nevada [2]. However, solar photovoltaic only provides 0.04% of the global energy usage. This is largely due to the high cost of making traditional crystalline silicon solar cells, which represents ∼90% of the world PV market just a few years ago. Continuous efforts in lowering the cost of solar photovoltaic make the thin film technology more and more popular. Today, the market share of thin film solar cell (mainly by First Solar) is near 20%.

An emerging third generation of photovoltaic technology, organic photovoltaic (OPV), provides promise of a low cost solar photovoltaic solution and attracts significant academic and industry research. The low cost of OPV comes from several intrinsic advantages of this technology: (a) organic materials are abundant; progress in organic chemistry forms a solid base for material innovation; (b) OPV materials have much higher absorption coefficients than silicon, which leads to typical OPV active layer thickness in the hundreds of nanometer range, resulting in low material consumption; (c) solution processable polymer OPV is compatible with high speed coating/printing technologies, which has a high material utilization efficiency; (d) the room temperature manufacturing process significantly reduces the energy input for solar cell production. In addition, OPV product is non-toxic and environmentally friendly. OPV also has the advantages of low specific-weight, mechanical flexibility and easy tunability of chemical properties of the organic materials, which enables multiple color and semi-transparent solar cells [3–5].

The power conversion efficiency (PCE) of OPV has been a big hurdle for the technology. Figure 1 shows the NREL certified OPV champion cell efficiency from 2001 (data was extracted from NREL Best Research-Cell Efficiencies Chart), which was still below 6% in 2008. Significant improvement was achieved in 2009, when the 7% PCE barrier was broken [6–11]. In July 2010, Solarmer Energy Inc. reported NREL certified 8.13% in single layer polymer solar cell, indicating OPV entered 8% era. In November 2010, Heliatek GmbH and Institute of Applied Photophysics (IAPP) showcased certified efficiency record of 8.3% with tandem structure in small molecule OPV system [12]. These recent progresses are significant events, and will further facilitate the pace toward commercialization of this technology.

Unlike inorganic semiconductor materials, organic semiconductor materials are characterized by significantly larger exciton binding energy of several tenths of electron volts (eV), resulting from a much lower dielectric constant. Upon the absorption of light, strongly-localized electron-hole pair or Frenkel excitons are formed. The tightly bonded excitons cannot be efficiently dissociated by an external electric field only. A breakthrough came in 1979, when Tang invented planar two layer organic photovoltaic cell using copper phthalocyanine (donor)/perylene tetracarboxylic derivative (acceptor) heterojunction structure. The paper was later published in 1986 [13]. Relatively high efficiency of ∼1% was achieved, which was far superior to that of early works of single layer OPV. The donor/acceptor interface was believed to be the site of exciton dissociation, and it was later recognized that the energy level difference of donor

**Corresponding author:** Jinsong Huang, E-mail: jhuang2@unl.edu.

Received: September 6, 2010. Accepted: January 7, 2011.

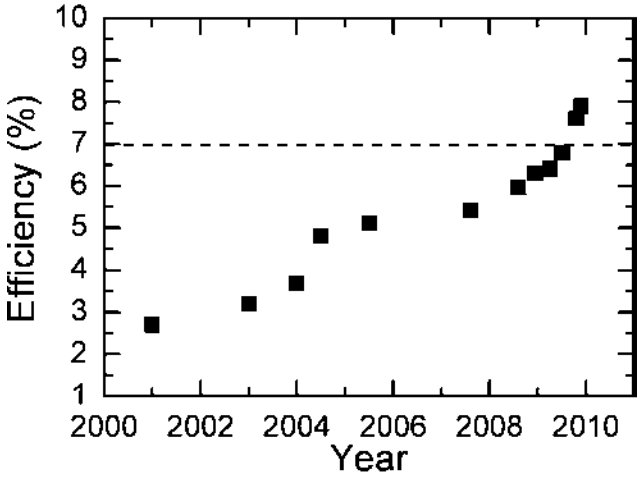


**Figure 1.** Certified champion power conversion efficiency of organic solar cells from 2001.

and acceptor provides the driving force of the dissociation. The application of the donor and acceptor mixture, or bulk-heterojunction (BHJ), in OPV was first demonstrated by Hiramoto in a three layer p-i-n structure, where the i-layer was realized by vacuum co-deposition of metal-free phthalocyanine $H_2$ PC (donor) and another perylene pigment Me-PTC (acceptor) [14, 15].

In the polymer side, Yoshino and coworkers first demonstrated the doping effect of fullerene (C60) in poly(3-alkylthiophnene) (PAT) in early 1992 by blending PAT and C60 [16]. Significant photoluminescence (PL) suppression/quenching was observed upon doping, and electron transfer from polymer chain to $C_{60}$ was later demonstrated [17, 18]. In the same year, Sariciftci et al. independently demonstrated photo-induced electron transfer from poly[2-methoxy,5-(2'-ethyl-hexyloxy)-p-phenylene vinylene] (MEH-PPV) and $C_{60}$ buckyball composite [19]. They then demonstrated MEH-PPV and $C_{60}$ double layer heterojunction devices (diodes, photodiodes and PV cells) in 1993. This is also an important period of polymer development for OPV application. Two teams, lead by Rieke and McCullough, invented regioregular head-to-tail coupled poly(3-alkylthiophene) (RR-P3AT) [20–22] using two different synthesis routes. Regioregular poly(3-hexylthiophene-2,5-diyl) (RR-P3HT) has been the focus point of high efficiency polymer solar cells and has only been surpassed in the last couple of years. Efficient bulk heterojunction polymer solar cells were later realized by UCSB and Cambridge groups in 1995 in polymer/fullerene [23] and polymer/polymer [24] systems independently. Currently, the high efficiency polymer solar cell systems are dominated by polymer/fullerene material combination. The invention of $C_{60}$ derivative [6,6]-phenyl-$C_{61}$-butyric acid methyl ester (PCBM) [25] by Wudl et al. represents a milestone in the development of polymer solar cells.

Because of the strong exciton binding energy in organic materials, organic solar cells work differently than inorganic solar cells. The energy conversion, or photovoltaic, process in organic solar cell can be separated into a multiple step process [26]. The overall external quantum efficiency $\eta_{\text{ext}}$ is a product of four parameters: absorption (A), exciton diffusion (ED), charge separation (CS) and charge collection (CC):

$$\eta_{\text{EXT}}(\lambda) = \eta_{\text{A}}(\lambda) * \eta_{\text{ED}}(\lambda) * \eta_{\text{CS}}(\lambda) * \eta_{\text{CC}}(\lambda)$$

The charge collection process involves both charge transport within the organic active layer (which is strongly related to the active materials, and the morphology [27–31] of each in multilayer cell or the blend in bulk heterojunction cell), as well as the charge extraction from the active organic layer to the electrodes. The extraction efficiency enhancement is a typical device engineering problem. In single layer polymer solar cell, research on the interface has led to inverted polymer solar cells [32] by introducing proper n- and p-type interfacial layers which can be reversed to change the polarity of the solar cell.

Utilizing multiple junction architecture, light harvesting of different parts of the solar spectrum can be realized. The highest recorded solar cell efficiency using III-V semiconductor is 41% PCE tested under concentrated light condition. Tandem structure is also important for organic solar cell research; with the efficiency always being a critical parameter, Brabec et al. performed an analysis on tandem OPV and claimed 15% PCE [33] is possible, compare to 10% PCE limit of single layer BHJ OPVs. Generally speaking, small molecule based OPV typically use a thermal evaporation approach for manufacturing, this method makes building tandem structures easier. However solution processable polymer tandem solar cells have also achieved significant progress within the last few years. This manuscript will focus on the intermediate layer(s) which enables the function of the tandem solar cell structure, for both small molecule and polymer based OPVs.

## 2 Review of Experimental Results

The design of the intermediate layer(s) structure is strongly influenced by the deposition methods of the subsequent subcells. For tandem devices with solution processed second or third subcells, the intermediate layer(s) should be designed to survive the subsequent solution coating. The intermediate layer(s) enabling thermal evaporated subsequent subcells are firstly reviewed. Then, the intermediate layer(s), enabling solution processed subsequent subcells are reviewed. Finally, some novel tandem OPVs with special intermediate layer(s) are discussed.

### 2.1 Intermediate Layer(s) for Small Molecule Based Subsequent Subcells

#### 2.1.1 Metallic Intermediate Layer

In 1990, Hiramoto et al. reported the first tandem OPV device [34]. The device consisted of two combined subcells, both of the subcells consisted of 50 nm of $H_2Pc$ and 70 nm of perylene tetracarboxylic derivative (Me-PTC). An ultrathin layer of gold (Au) was inserted between the two units by vacuum deposition, as shown in Figure 2. The open circuit voltage ($V_{oc}$) of the tandem devices was 0.78 V, which is a 77% increase in voltage when compared to a single cell (0.44 V). For a tandem device without the Au layer inserted between the two units, the $V_{oc}$ was even lower than that of a single cell. This result shows that the $V_{oc}$ can be sufficiently improved by the concept of stacking two cells in series.

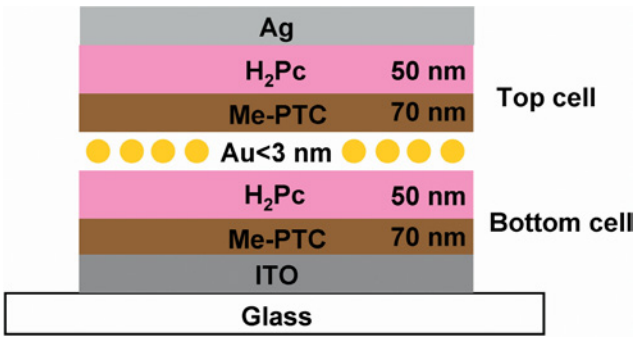


**Figure 2.** Schematic structure of the first tandem organic solar cell demonstrated by Hiramoto et al. [34]. An ultrathin layer of Au clusters were used as intermediate layer.

In 2002, Yahimov and Forrest demonstrated high photovoltage by stacking two, three or five heterojunction cells in series [35]. Each individual cell consisted of copper phthalocyanine (CuPc) as a donor, and 3,4,9,10-perylene tetracarboxylic bis-benzimidazole (PTCBI) as an acceptor: see Figure 3. In their work, an ultra-thin (∼0.5 nm average thickness) layer of silver (Ag) clusters were used as an intermediate layer to serve as recombination centers. The maximum PCE of the optimized two-junction and three-junction device was 2.5% and 2.6%, respectively, which were much higher than the maximum PCE of a corresponding single cell (1.1%). The $V_{oc}$ of these tandem cells at one sun illumination were 0.93 V and 1.20 V for two and three junction devices, respectively. Meanwhile, the five-junction device showed low efficiency (∼1%) at one sun illumination, and the $V_{oc}$ (1.73 V) was lower than the expected value (2.3 V).

In both Hiramoto's [34] and Yahimov's [35] research, ultra-thin inert metal layers were used as an intermediate layer. It's worth noting that, the $V_{oc}$ of the tandem device reaches its maximum value when the ultra-thin metal layer (∼0.5 nm) is far from continuous. Yahimov suggested that the metal clusters induce defects in the PTCBI energy gap. The gap states serve as recombination centers and prevent the cell from being charged. However, the gap states are suggested to be not as efficient as metal clusters in recombining the charges due to its low charge carrier capture cross section [35].

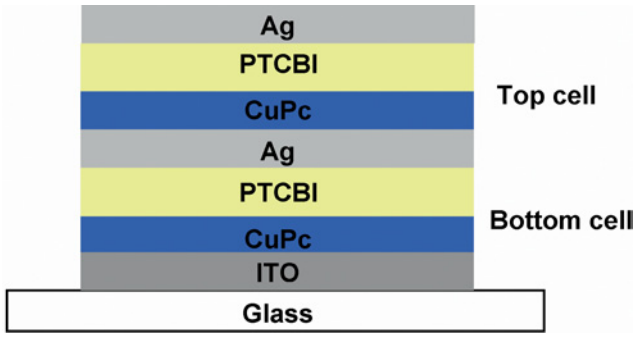


**Figure 3.** Schematic structure of the tandem organic solar cell demonstrated by Yahimov et al. [35]. An ultrathin layer of Ag clusters were used as intermediate layer.

For the tandem devices with Ag clusters as the intermediate layer, further research has been carried out in the followed years to understand the influence of the Ag cluster on device performance. In 2004, Rand et al. investigated the optical properties of the silver clusters and provided an explanation for the previous observation that the PCE of tandem device was improved by a factor of more than two, as compared to that of a single cell [26, 36]. The optical field near the Ag clusters was enhanced by the surface plasmon resonance and the scattering of photons supported by Ag clusters. The enhanced incident optical field persists into the organic layer for a distance of about 10 nm, allowing for an increased absorption within the thin organic film near the Ag cluster array. The plasmon enhanced absorption is helpful in some material systems with small exciton diffusion length, such as CuPc and PTCBI, where the active layer usually has to be thin, and hence the absorption of the light is not complete.

The Ag nanocluster layer was later applied to tandem devices with two BHJ by Xue et al. [37]. The BHJ is a mixture of CuPC and $C_{60}$, and the structure of the device is shown in Figure 4, where PTCBI and bathocuproine (BCP) were used as the exciton-blocking layer. In this study, the PCE was reported to be 5.7% under one sun condition, which was about 15% higher than that of a single cell. A maximum PCE of 6.5% was suggested in their work if the layer thickness were optimized.

Interestingly, in these tandem devices with a metallic intermediate layer, the $V_{oc}$ of tandem devices are almost the sum of the $V_{oc}$ of each subcells despite the cathode and anode of the top cell consisting of same metals (Au or Ag). Similar phenomenon has been observed in several other studies [38]. Although the work function difference between the anode and cathode may limit the $V_{oc}$ of solar cells, the "Au/organic/Au" or "Ag/organic/Ag" structure for these

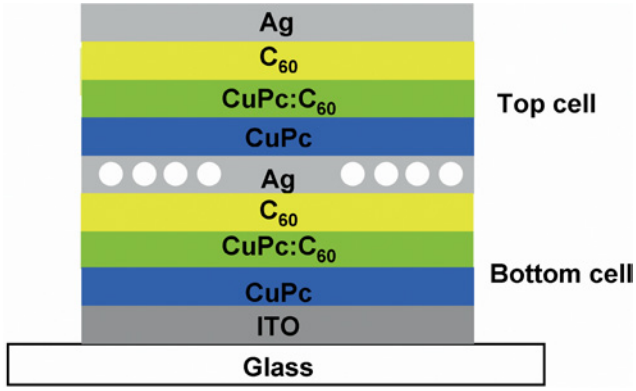


**Figure 4.** Schematic structure of tandem organic solar cell based on BHJ as active layer demonstrated by Xue et al. [37].

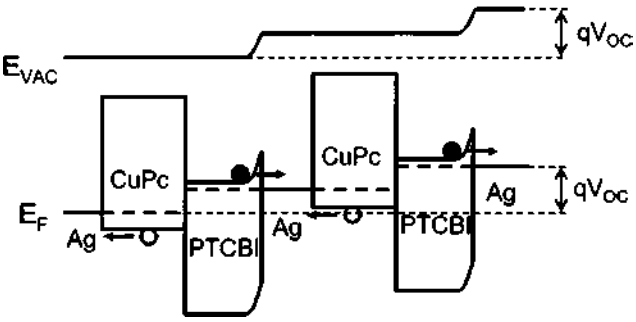


**Figure 5.** Energy level diagram of the tandem devices with Ag intermediate layer proposed by Peumans et al. [26].

cases works well. Peumans et al. proposed that dipoles may be formed in organic/metal interfaces at both the anode and cathode [26], as illustrated in Figure 5. In this scenario, the $V_{oc}$ is determined by the Fermi energy difference between the acceptor and donor materials. Interface dipoles between organic semiconductor and metal layers are frequently observed in organic optoelectronic research. The energy shift induced by the dipoles at the organic/metal interface can exceed 1.0 eV in some cases [39–41], which is large enough for the origin of $V_{oc}$.

One of the limitations of the metallic intermediate layer is caused by the diffusion of metal into the organic sublayer during thermal evaporation [37, 38]. This diffusion could lead to a small shunt resistance of the bottom cell reducing the fill factor (FF) of the whole device. Meanwhile, the metal atoms diffused into the active layer would damage the organic molecules and form charge traps. Besides, the low transparence nature of metal layers is another problem. E.g., a thin layer of Au or Ag with a thickness of 10 nm will lead to a transmission loss of about 40% [42] or 50% [43] at a wavelength of 550 nm, respectively. To reduce the optical loss by the metal layer, the thickness of the metal layer should be as small as possible.

### 2.1.2 Electrical Doped Intermediate Layer(s)

In optoelectronic devices based on organic semiconductors, controlled doping of the transport layers has been fully demonstrated to be an efficient way to achieve highly conductive transport layer and ohmic contacts at the organic/metal interface. Doping can improve the carrier concentration in the doping region by several orders of magnitude. The high carrier concentration leads to a very narrow space charge layers near the contact interface and results in a significantly reduced contact resistance by tens to hundreds of times [44, 45].

In 2004, Maenning et al. studied OPV devices with an active layer sandwiched between the n-doped and p-doped charge transport layers and demonstrated organic tandem devices based on multi-stacked p-i-n cells [46]. In their research, the active layer was a mixture of phthalocyanine zinc (ZnPc) and $C_{60}$ with a thickness of 30 nm. For the p-doping, tetra-fluorotetracyano-quinodimethane (F4-TCNQ) was used as acceptor, and the host material was N,-diphenyl-N,-bis(3-methyl phenyl)-[1,-biphenyl]-4,-diamine (MeO-TPD), which was found to be better than 4,4',4"-tris-(3-methylphenyl phenylamino) triphenylamine (m-MTDATA). For the n-doping, rhodamine B chloride was used as a precursor for a strong donor, the host for n-doping was $C_{60}$, which was the best choice among 1,4,5,8-naphthalenetetracarboxylic-dianhydride (NTCDA), N,N_-dimethyl-3,4,7,8-naphthalene-tetracarboxylic-diimide (Me-NTCDI) and C60. The conductivity of p-doped MeO-TPD and n-doped $C_{60}$ was $10^{-5}$ S/cm and $10^{-4}$ S/cm, respectively. A discontinuous Au layer (1.0 nm) was inserted between the two subcells. Several advantages of using p-i-n tandem solar cells were suggested. First, the transport layer is high conductive after doping, therefore the ohmic loss in the transport layers is negligible. The high conductivity enables thick transport layer to act as an optical spacing layer (Figure 6), so that the active layers of each single cell can be placed at the position with maximum optical field strength. Second, the electrically doped transport layer can form ohmic contacts with the Au layer which can avoid energy dissipation during the carrier recombination at the intermediate layers. In contrast to Yakimov's stacked cells [35], here the metal layer alone is not sufficient to form good electrical contact, and solely doping either side of contact layer adjacent to the Au layer was found to be not sufficient enough for high forward currents or for good fill factor. As expected, the $V_{oc}$ of the tandem device (0.85 V) was improved by an increase of 89% as compared to that of single device (0.45 V); the PCE of the tandem device was reported to be 2.4%, which is about 23% higher than that of a single cell.

Later, using electrically doped transport layer as an optical spacer for better light harvesting was further demonstrated by Drechs et al. [47]. As shown in Figure 7, the optimized structure results from the optical interfer-

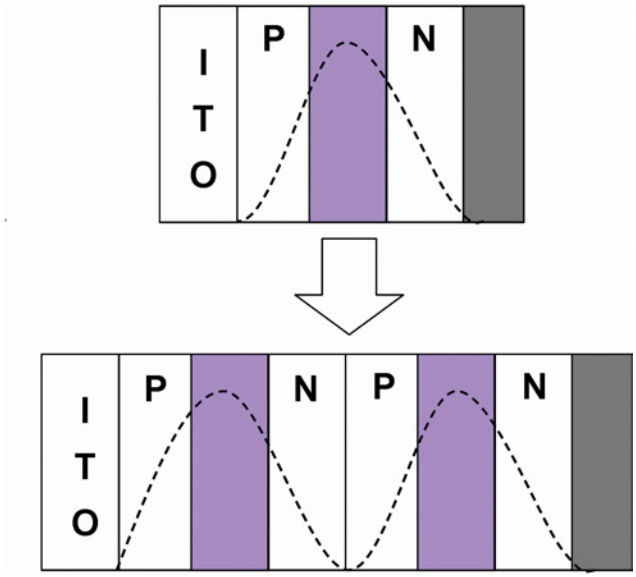


**Figure 6.** Schematic diagram of placing the active regions to the maxima of the optical field by using electrical doped wide band gap transport layer as optical spacer, demonstrated by Maenning et al. [46].

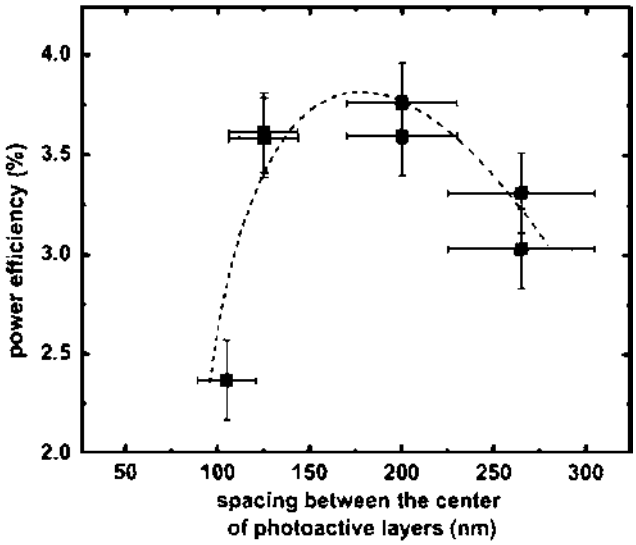


**Figure 7.** Power efficiencies for p-i-n tandem solar cells with different thickness of the spacing layer, demonstrated by Drechsel et al. [47].

ence effect and subcells balancing was indium-tin oxide (ITO)/p-doped MeO-TPD (30 nm)/ZnPc:$C_{60}$ (1 : 2, 60 nm)/n-doped $C_{60}$ (20 nm)/Au (0.5 nm)/p-doped MeO-TPD (125 nm)/ZnPc:$C_{60}$ (1 : 2, 60 nm)/n-doped $C_{60}$ (20 nm)/aluminum (Al). The $V_{oc}$ of tandem devices was 0.99 V which was doubled as compared to the single cell (0.50 V). The PCE of the tandem devices was 3.8% under 130 mW/cm$^2$ simulated AM 1.5 illumination, which was an 81% improvement when compared to a single device (2.1%).

In 2006, Colsmann et al. reported a tandem solar cell comprising of polymer and small-molecule subcells [48]. In their work, the intermediate layers consisted of two doped organic semiconductor layers and a thin Au metal layer. The n-doped layer is lithium doped 4,7-Diphenyl-1,10-phenanthroline (Bphen:Li, 8 nm); the p-doped layer is MTDATA: F4TCNQ (8 nm), and the thickness of Au metal layer is 10 nm: see Figure 8. The $V_{oc}$ of the tandem device was 0.99 V, which is close to the sum of the $V_{oc}$ of each subcells (0.57 V for polymer cell and 0.51 V for small-molecule cell, respectively). However, the PCE of the tandem device (1.2%) was even lower than that of the single polymer cells (1.5%). This was explained by the competition of photon harvesting in both cells due to the spectral overlap. Besides, the low transparency of the 10 nm Au layer may be another reason. In this work, the usage of a doped layer on both sides of the Au layer was also suggested to be mandatory for the operation of the tandem cells. The $V_{oc}$ of all the devices without the doped layer were found to be significantly lower than the sum of the individual cells [48].

### 2.1.3 All Organic Intermediate Layer(s)

All organic intermediate layers provides advantages such as excellent optical properties, avoiding metal cluster diffusion into photo active layers and easing of fabrication by thermal evaporation. Since the conductivity of the transport layer is significantly improved by electrical doping, it is worthwhile to identify whether the doped intermediate layers can work well without an ultra-thin metal layer.

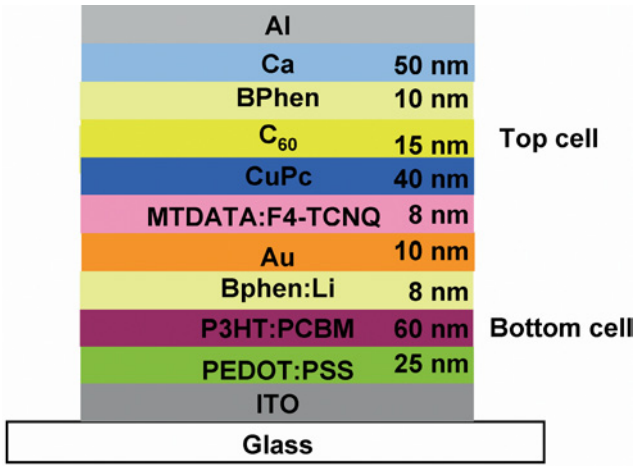


**Figure 8.** Schematic structure of tandem organic solar cell comprising polymer and small-molecule subcells demonstrated by Colsmann et al. [48].

In Maenning's work, the tandem device without an Au layer showed a lower forward current and a reduced fill factor (from 0.45 to 0.32) [46]. The Au interlayer was proposed to play a dual role. On one hand, it may hinder the interdiffusion of dopants, which would otherwise lead to compensated region. On the other hand, it provides gap states that assist the tunneling charges through the p-n junction barriers. But recently, Schueppel et al. reported p-i-n tandem solar cells with metal-free intermediate layers [49]. In this work, the commonly used p-dopant F4-TCNQ and n-dopant acridineorange base (AOB) was replaced by NDP9 and NDN1 because of their better processability. The structure of the intermediate layers was C60: NDN1 (2 wt %, 5 nm)/N,N'-diphenyl-N,N'-bis(4'-(N,N-bis(naphth1yl)-amino)-biphenyl-4-yl)-benzidine (DiNPB): NDP9 (10 wt %, 5 nm) DiNPB: NDP9 (5 wt %, 0–186 nm): see Figure 9. The heavily doped DiNPB layer was used for recombination contact. With this architecture a fill factor of about 59%, a $V_{oc}$ of 1.06 V and a PCE of 3.8% was observed in an outdoor measurement.

In 2008, based on a much different conception, Yu et al. reported a kind of tandem solar cell with an all organic tunnel junction as the intermediate layer [50]. In their work, a heterojunction of tin dicholophthalocyanine ($SnCl_2Pc$) (3 nm)/copper hexadecafluorophthalocyanine ($F_{16}CuPc$) (3 nm) was used between two solar cells with ZnPc and $C_{60}$ as an active material. The structure of the device can be seen in Figure 10. The $V_{oc}$ of the tandem device (1.04 V) was reported to be double that of the single cell (0.54 V). The PCE increased from 1.11% to 1.46%. From the author's opinion, the carrier concentration at the heterojunction interface of these non-doped organic films was much higher than that in bulk. The author proposed the anisotype heterojunction makes the electron flow from both $SnCl_2$ Pc and ZnPc layer to $F_{16}$ CuPc layer by thermal emission. The high electron density accumulated in the F16CuPc layer was proposed to improve the tunneling probability at the $F_{16}$CuPc/ZnPc interface.

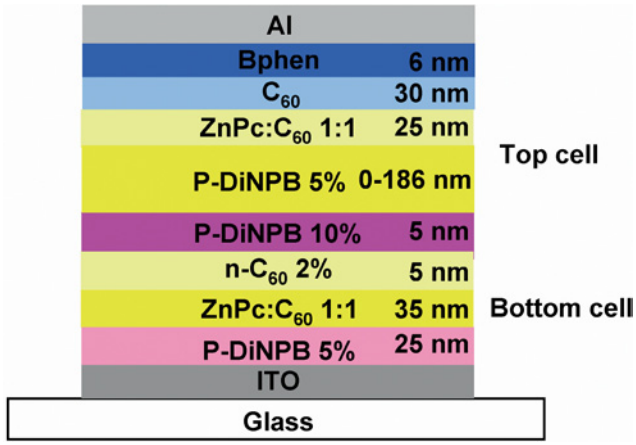


**Figure 9.** Schematic structure of tandem organic solar cell with all organic intermediate layers demonstrated by Schueppel et al. [49].

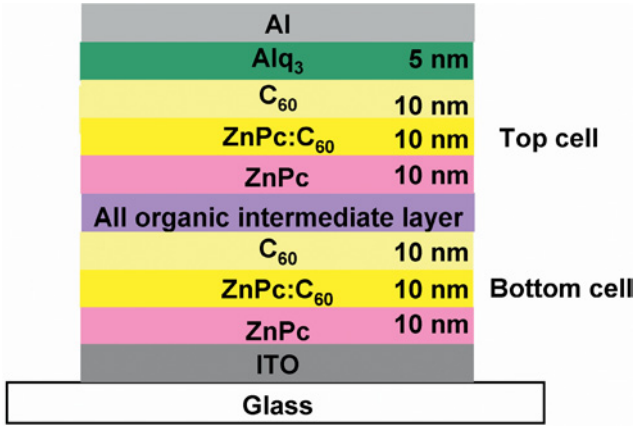


**Figure 10.** Schematic structure of tandem organic solar cell with all organic intermediate layers demonstrated by Yu et al. [50], the organic intermediate layers were $F_{16}CuPc$, $SnCl_2Pc$ or $SnCl_2Pc/F_{16}CuPc$, respectively.

#### 2.1.4 Metal Compound Based Intermediate Layer(s)

Metal compounds including n-type-like compounds such as lithium fluoride (LiF) [41, 51], cesium fluoride (CsF) [52, 53], cesium carbonate ($Cs_2CO_3$) [54–59] and p-type-like metal oxides such as molybdenum oxide ($MoO_3$), tungsten oxide ($WO_3$), vanadium oxide ($V_2O_5$) have received considerable attention in the organic optoelectronic research in organic transistor [56], OPV [32, 60–63] and organic light-emitting devices (OLEDs) [64, 65] due to their highly efficient charge injecting (or extracting) properties, improved stability, high transparence and compatible easy-fabrication process (thermal evaporation). So far, intermediate layer(s) with metal compound as the injection layer have been widely reported in tandem OLEDs [66–68].

In 2007, Janssen et al. reported small molecule and polymer tandem OPV device with intermediate layers of LiF (0.5 nm)/Al (1.0 nm)/$WO_3$ (3 nm) [42], the high-work function $WO_3$ layer was shown to be more promising than an Au layer. The structure of the tandem device is shown in Figure 11. In their work, the thicknesses of the $WO_3$ layer (3 nm) and Au layer (10 nm) have been optimized. However, the Au film show a transmission of only about 50% in the spectral region from 400 nm to 600 nm, while the transmission of $WO_3$ in the same wavelength region was more than 95%. Numerical simulation showed that the intensity of the light that overlaps with the top cell can be increased by 50% by using $WO_3$. The electrical contact between the intermediate layers and the top cell have not been discussed in detail, but the $WO_3$ is believed to able to form ohmic contact with CuPc due to the high work function of $WO_3$ (reported to be ~5.3 eV [56] to

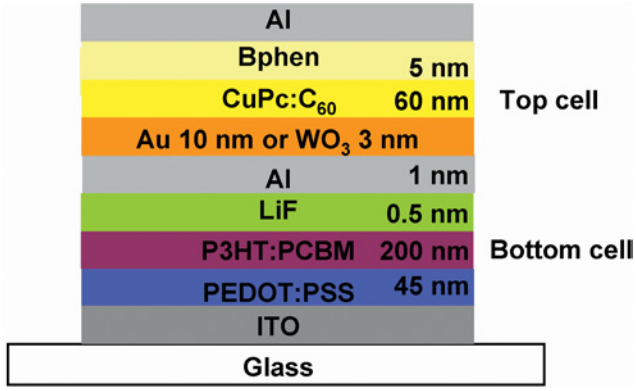


**Figure 11.** Schematic structure of tandem organic solar cell with Al/Au or Al/$WO_3$ as intermediate layers demonstrated by Janssen et al. [42].

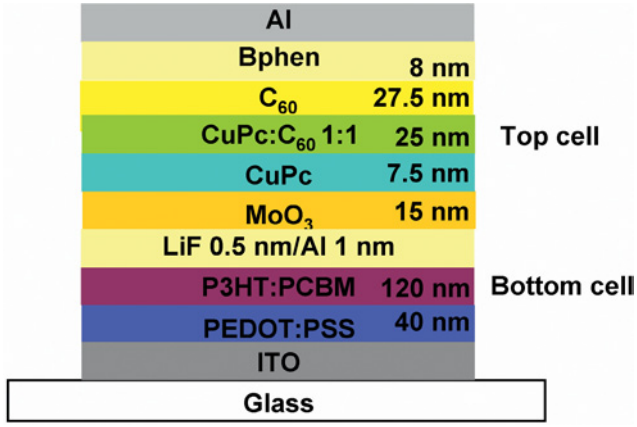


**Figure 12.** Schematic structure of tandem organic solar cell with LiF/Al /$MoO_3$ as intermediate layers demonstrated by Zhao et al. [69].

6.4 eV [64]), which is larger than Au (5.2 eV) and the highest occupied molecular orbital (HOMO) of CuPc (5.2 eV). The $V_{oc}$ of tandem device was about 0.6 V, which is less than the sum of the $V_{oc}$ of the subcells (0.40 V and 0.43 V for small molecule and polymer subcells respectively), this was attributed to the imperfect contact between the LiF/Al layers and the polymer subcell. The PCE of tandem device with 3 nm $WO_3$ was found to be about 0.5% higher than that of tandem device with 10 nm Au layer, at an illumination of 16 to 160 mW/cm$^2$. A PCE of about 4.6% was obtained at 16 mW/cm$^2$ by the use of $WO_3$.

Later, Zhao et al. reported similar tandem OPV devices with LiF (0.5 nm)/Al (1 nm)/$MoO_3$ (15 nm) intermediate layers [69]: see Figure 12. The transmittance of the intermediate layers was about 98%. The bottom cell was a polymer cell based on P3HT:PCBM, the top cell was small molecule cell based on CuPC:$C_{60}$. The tandem cell here achieved a $V_{oc}$ of 1.01 V, short circuit current density ($J_{sc}$) of 6.05 mA/cm$^2$ and a FF of 46%, resulting in a PCE of 2.82%. The $V_{oc}$ is close to the sum of the polymer cell (0.63 V) and the small molecule cell (0.45 V), demonstrating that the LiF/Al/$MoO_3$ intermediate layers form good contact with both the two subcells. The high work function of $MoO_3$ matches well with the HOMO of CuPc (5.2 eV). In their work, the $MoO_3$ was proposed to behave as an exciton blocking layer because the band gap of $MoO_3$ (3.0 eV) is larger than that of CuPc (1.7 eV) and P3HT (1.9 eV) [70]. This will be more attractive if the exciton blocking effect of $MoO_3$ can be confirmed by experiments. It is noticeable that Zhao also demonstrated tandem solar cells with two solution processed polymer subcells using Al/$MoO_3$ as intermediate layers, which will be discussed below.

Although the p-type and n-type metal compound can form ohmic contact with organic cells, so far no results have demonstrated that the ultra-thin metal layer between the metal compound layers can be omitted. Lately, Chen et al. reported tandem solar cells with intermediate layers of $Cs_2CO_3$ (0.5 nm)/Ag (1.5 nm)/$MoO_3$ (3 nm) [71]. In this work, the $V_{oc}$ and PCE of tandem device were shown to decrease evidently when the thin Ag layer was omitted (from 1.21 V to 0.65 V). In previous work [56, 57], it was demonstrated that the formation of ohmic contact at the "organic/$Cs_2CO_3$/metal" interface is strongly dependent on the formation of "Cs-O-metal" complex. This complex provides a strong dipole between the organic layer and the electrode, which makes the Fermi level of the electrode shift toward the lowest unoccupied molecular orbital (LUMO) of organic materials. From this point of view, an Ag layer was required in the case of $Cs_2CO_3$ (0.5 nm)/Ag (1.5 nm)/$MoO_3$ (3 nm) intermediate system. In the cases of devices employing LiF or CsF as interlayer, a metal layer is also required [41, 42, 69, 72, 73]. The working principles of LiF and CsF have been reviewed by Hung [41]. Besides, a compensated region was proposed when the n-type metal compound contacts the p-type metal compounds, which could be another reason for the requirement of metal layer. [46]

### 2.2 Intermediate Layer(s) for Polymer Based Subsequent Subcells

Small molecule based OPV typically uses the thermal evaporation approach for fabrication, so the realization of tandem structures is relatively easier. However, the solution processed polymer OPV, intermediate layers are required to protect the bottom cells. Besides, the wettability of the solutions on the existing layer is another practical problem to be addressed. Despite this, there has been significant progress for solution processed polymer tandem solar cell in the last few years.

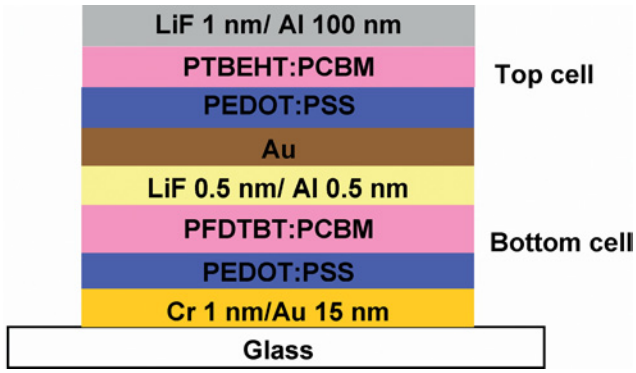


**Figure 13.** Schematic structure of the first tandem organic solar cell consisted of two solution processed subcells by Hadipour et al. [74].

#### 2.2.1 Thermal Evaporated Metal and Metal Compound Based Intermediate Layer(s)

The first tandem cell consisted of two solution processed subcells with complementary absorption was reported by Hadipour et al. [74]. In their study, composite intermediate layers were applied to serve as both an ohmic contact electrode and a protecting layer in the subsequent spin coating process. The intermediate layers were LiF (0.5 nm)/Al (0.5 nm)/Au (15 nm)/poly(3,4-ethylenedioxythiophene) oxidized with poly(4-styrenesulfonate) (PEDOT:PSS) (60 nm). The LiF/Al was used to form ohmic contact with PCBM and the Au/PEDOT:PSS was used to form ohmic contact with poly{5,7-di-2-thienyl-2,3-bis(3,5-di(2-ethylhexyloxy)phenyl)-thieno [3,4-b]pyrazine} (PTBEHT). The bottom cell consisted of poly((2,7-(9,9-dioctyl)-fluorene)-alt-5,5-(4′,7′-di-2-thienyl-2′,1′,3′-benzothiadiazole) (PFDTBT) and PCBM in a 1 : 4 ratio, the top cell consisted of PTBEHT and PCBM in a 1 : 4 ratio, the structure of the device is shown in Figure 13. All polymers were dissolved in chloroform. The damaging of LiF/Al by water-based PEDOT:PSS was prevented by the continuous Au layer (10–15 nm). As expected, a high $V_{oc}$ of 1.4 V was achieved, which was the sum of the $V_{oc}$ of the bottom cell (0.9 V) and the top cell (0.5 V). The PCE of the tandem cell was 0.57%, which is close to the sum of the PCE of each single cell (0.35% and 0.23%, respectively). In this work, the smallest thickness of the Au layer was 10–15 nm. Due to the two semitransparent metal electrodes, the bottom cell forms an optical cavity. In order to improve the transmission of the bottom cell in the wavelength range of 700 to 950 nm (absorption peak of top cells), the thickness of the bottom cell had to be optimized.

In 2008, Zhao et al. showed an alternative approach to protect the bottom cell from being dissolved. They used a thick $MoO_3$ layer as a protecting layer [69]. The intermediate layer consisted of Al (1 nm)/ $MoO_3$ (15 nm). The active layer of both subcells was a P3HT:PCBM layer, and the solvent was chlorobenzene. The $V_{oc}$ of the tandem device was 1.17 V, resulting in an 86% improvement when compared to a single cell. However the PCE of tandem device (2.2%) was similar to that of the single cells (1.9% and 2.4%, respectively), because the $J_{sc}$ of the tandem device ($<4$ mA/cm$^2$) was lower than that of a single cell (about 5–6 mA/cm$^2$). In 2009 Zhao et al. demonstrated a triple-tandem solar cell with the same intermediate layers and active layers, where the $V_{oc}$ (1.73 V) was almost triple that of a single cell (0.62 V) [75].

#### 2.2.2 Zinc Oxide Based Intermediate Layer(s)

A significantly progress was made by Gilot et al in 2007. By introducing a solution processed zinc oxide (ZnO) into organic tandem solar cell, Gilot et al. realized fully solution processed tandem solar cell for the first time [76]. A ZnO electron transport layer was combined with a neutral PEDOT:PSS layer as the intermediate layer, with the structure of the tandem device shown in Figure 14. The ZnO nanoparticles were spin coated from an acetone solution to form a 30 nm thick layer. The electron mobility of the solution processed n-type ZnO layer was reported to be as high as 0.066 cm$^2$V$^{-1}$s$^{-1}$ [77]. Since ZnO could be dissolved by the water based acidic PEDOT:PSS, the PEDOT:PSS was modified to a neutral pH level. Electron donors P3HT or poly[2-methoxy-5-(3',7'-dimethyloctyloxy)-*p*-phenylene vinylene] (MDMO-PPV) was mixed with electron acceptor PCBM and was spin coated from a chlorobenzene solution to form an active layer. The ZnO/PEDOT:PSS intermediate layer did not damage the bottom cell and was able to protect it during the subsequent spin coating process of the top cell. This is an efficient and practical method to manufacture multiple junction all solution processed polymer solar cells. For demonstration, the author also fabricated tandem solar cell consisting of three subcells with a $V_{oc}$ of 2.19 V. For the two cells tandem OPV device with MDMO-PPV:PCBM as the bottom cell and P3HT:PCBM as the top cell, the $V_{oc}$ (1.34–1.38 V) was less than the sum of that of two single cells (0.75–0.84 V). The authors attribute this to the non-ohmic contact ZnO/PEDOT:PSS interface. In their work, the $V_{oc}$ was improved to 1.53 V by exposing the ZnO layer to UV light, which can be explained by the increase in charge carrier concentration within the ZnO layer after the photo-doping process [78, 79]. A similar improvement was observed when the Ag metal cluster was used at that interface. This all solution processed multijunction solar cell is a promising big step for practical applications. Recently, Gilot et al. improved the tandem OPV device to 4.9% PCE with ZnO/neutral PEDOT:PSS as the intermediate layer [80].

The use of ZnO combined with PEDOT:PSS requires a pH neutral PEDOT:PSS. Recently however, Moet et al. suggest the neutralization process will lead to a reduced work function of the PEDOT:PSS [81]. In their work, the acidity

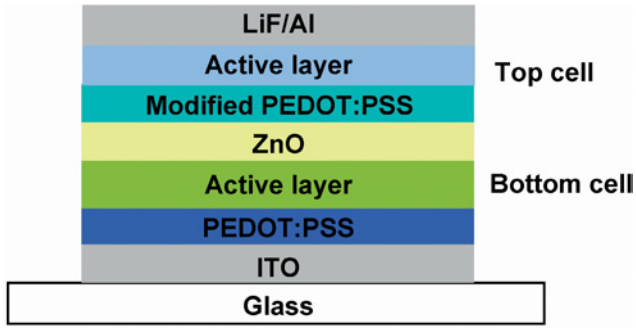


**Figure 14.** Schematic structure of the tandem organic solar cell with ZnO based intermediate layers demonstrated by Gilot et al. [76]. For the active layers, thin films of a blend of P3HT:PCBM (1 : 1) and MDMO-PPV:PCBM (1 : 4) were used.

of the highly conductive PEDOT:PSS dispersion (Clevios PH500, PEDOT:PSS ratio 1 : 2.5 by weight, H. C. Starck) was modified systematically by the addition of a 1 : 8 dilution of 2-dimethylaminoethanol (DMAE, Aldrich) in water. It was found that the work function of the 45 nm PEDOT:PSS film decreased by 0.5 eV when the acidity changed from a pH level of 1.9 to a pH level of about 2.5, and then it showed a further decrease of about 0.2 eV when the acidity changed to pH level of 7. When poly[9,9-didecanefluorenealt-(bis-thienylene) benzothia diazole] (PF10TBT) mixed with PCBM was used as an active layer in the subcells, the $V_{oc}$ of the tandem device with the neutral PEDOT:PSS (1.5 V) was less than expected (2 V). The reduced $V_{oc}$ was directly attributed to the reduced work function of PEDOT:PSS. Moet reported a method to recover the work function of PEDOT:PSS in their work. A pure Nafion layer was spin coated on top of the PEDOT:PSS layer to form a ultra-thin layer of mixture of Nafion and PEDOT:PSS, which had an improved work function of 5.7 eV [82]. This ultra thin acid mixture layer (pH 3.4) was blocked by a neutral PEDOT:PSS layer and hence would not damage the underlying ZnO layer. The tandem device with reformulated ZnO/PEDOT:PSS intermediate layers exhibited a improved $V_{oc}$ of 1.92 V and a FF of 0.61, demonstrating an ohmic contact at the PEDOT:PSS/PF10TBT interface.

#### 2.2.3 Titanium Oxide Based Intermediate layer(s)

In 2007, Kim et al. reported a highly efficient tandem solar cell with titanium oxide ($TiO_x$)/PEDOT:PSS as intermediate layers [83]. It is considered a breakthrough in solution processed tandem solar cell research with a PCE of 6.5% being reported. The inorganic $TiO_x$ layer can form barriers against physical or chemical damage during the subsequent solution processing, and it is robust to slow down the permeation of oxygen and moisture. In contrast to ZnO nanoparticles, the $TiO_x$ layer is insensitive to the acidity of the PEDOT:PSS. It provides large freedom in the design of solution processed multijunction devices. The $TiO_x$ layer was fabricated by a low temperature sol-gel process (a temperature of 150 ˚C was required for annealing), which is compatible with the annealing of the polymer:PCBM blends. The Ti : O ratio studied by XPS was found to be 1 : 1.34 and the electron mobility of this $TiO_x$ film was about $1.7 \times 10^{-4} cm^2 V^{-1} s^{-1}$ [70]. The LUMO (conduction band) and HOMO (valence band) of the $TiO_x$ film is 4.4 eV and 8.1 eV, respectively. The large bandgap of the $TiO_x$ allows it behaviors as an excellent hole and exciton blocking layer. The cross section transmission electron microscopy images of the polymer tandem solar cell show that there is no interlayer mixing (Figure 15). In their work, low bandgap polymer poly[2,6-(4,4-bis-(2-ethylhexyl)-4H-cyclopenta[2,1-b;3,4-b'] dithiophene)-alt-4,7-(2,1,3-benzothia diazole)] (PCPDTBT) mixed with PCBM was used as the active layer of the bottom cell, the P3HT: PCBM was used as the active layer of the top cell. The two subcells possess complementary absorption spectrums from 300 nm to 900 nm. As expected, Kim et al. achieved a tandem device with a $V_{oc}$ of 1.24 V, $J_{sc}$ of 7.8 $mA/cm^2$, and a FF of 0.67, result in a PCE of 6.5%.

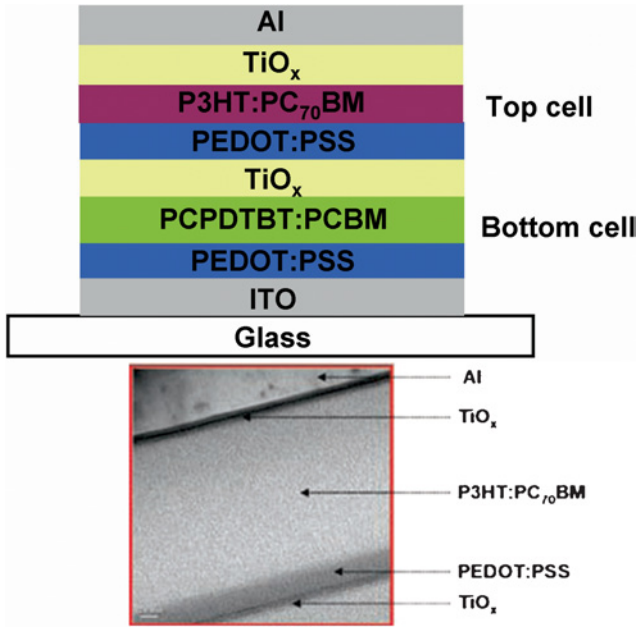


**Figure 15.** Schematic structure of the highly efficient tandem organic solar cell with TiOx based intermediate layers demonstrated by Kim et al. [83].

Similar to ZnO/PEDOT:PSS interface, the $TiO_x$/PEDOT:PSS intermediate layer was found to be non-ohmic contact. Sista el al. have studied tandem solar cells with Al (0.5 nm)/$TiO_x$ (20 nm)/PEDOT:PSS (50 nm) intermediate layers and found that the devices show a significant S-shape near the $V_{oc}$ point [84]. Previous research

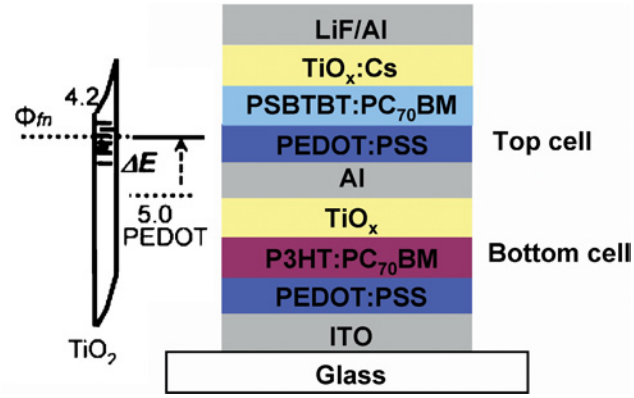


**Figure 16.** Schematic structure of tandem organic solar cell with TiOx based intermediate layers demonstrated by Sista el al. [84].

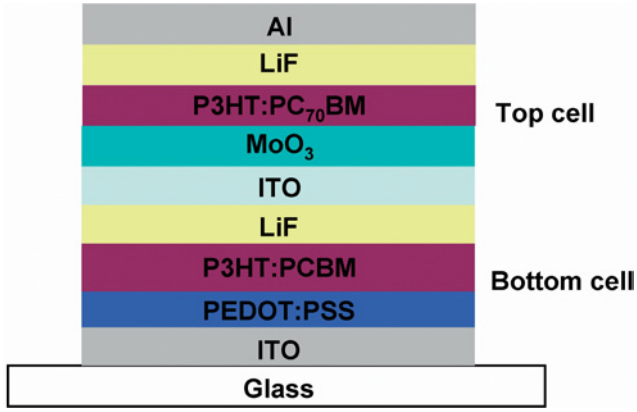


**Figure 17.** Schematic structure of tandem organic solar cell with sputtered ITO layer as intermediate layers demonstrated by Sakai et al. [95].

revealed that the S-shape curve could be derived from an interfacial barrier [85]. However, when the device was illuminated with UV photons, the S-shape disappears. The UV-induced Schottky-to-Ohmic transition was explained as follows: the PEDOT:PSS (VP AL 4083 from H. C. Stark) is a heavily p-doped conducting polymer and hence can be considered as a metal, therefore the $TiO_x$/PEDOT:PSS interface forms a typical triangular barrier, as shown in Figure 16. A wide triangular barrier resulting from the relatively low carrier concentration of the pristine $TiO_x$ layer hinders the charge extraction and leads to an S-shape curve. After exposure to UV light, the free carrier concentration in the $TiO_x$ layer increased significantly, leading to a much narrowed triangular barrier width. In this situation, the tunneling of electrons through the thin barrier becomes efficient and the $TiO_x$/PEDOT:PSS contact turns to be ohmic.

It is worth noting that, in Sista's work [84], a 10 nm layer of $TiO_x$:Cs was inserted between the Al cathode for a more efficient electron extraction. In 2009, Park et al. reported Cs-doped anatase $TiO_x$ layer and obtained an improved polymer/electrode contact in both polymer solar cell and light emitting devices by the use of the $TiO_x$:Cs layer [86]. The $TiO_x$:Cs layer was fabricated by mixing a $Cs_2CO_3$ solution with a nanocrystalline $TiO_x$ solution, where the nanocrystalline $TiO_x$ was synthesized by the sol-gel process [87]. XPS studied showed that there is a charge transfer between the $TiO_x$ and the Cs. As a result the LUMO of $TiO_x$ is modified from 4.2 eV to 3.9 eV by Cs-doping, which is more desirable for efficient electron extraction.

#### 2.2.4 Sputtered Intermediate Layer(s)

As a widely used transparent conducting material, ITO was also used as an intermediate layer. However, traditional RF sputtering processes of ITO damages the underlying organic layers by the bombardment effect of the energetic particles as well as high temperature. Despite this, sputtering ITO or indium-zinc oxide (IZO) on organic layers has been achieved in organic light emitting device research [88–93] by using low plasma power density at room temperature, and by restraining the bombardment effect as much as possible.

In 2006, Kawano et al. reported an organic tandem solar cell with ITO/PEDOT:PSS as intermediate layers [94]. The ITO layer was deposited by dc magnetron sputtering in 1 Pa argon without substrate heating. The argon in the chamber with a pressure of 1 Pa can reduce the bombardment effect [90, 91, 93]. The active layer of both the two subcells was poly[2-methoxy-5-(3',7'-dimethyloctyloxy)-1,4-phenylene vinylene] (MDMO-PPV) blended with PCBM with a ratio of 1 : 4. In their work, the device with 20 nm of ITO shows slightly better performance than the device with 100 nm of ITO, indicating that the 20 nm ITO is thick enough to prevent the bottom cell from dissolving. The $V_{oc}$ of the tandem device with 20 nm of ITO (1.34 V) was only 60% times higher than that of single device (0.84 V). The PCE of the tandem device was 3.1%, which was about 35% higher than that of a single device (2.3%). The reduced $V_{oc}$ was mainly attributed to the high work function of ITO (4.9 eV), which leads to an energy loss during the charge recombination at the PCBM/ITO interface. Recently, Sakai and Kawano modified the PCBM/ITO layer with 0.5 nm LiF [95]: see Figure 17. However the $V_{oc}$ of the tandem device (1.14 V) was still less than the sum of the $V_{oc}$ of each single cell (0.7 V and 0.58 V, respectively), showing that the 0.5 nm LiF can not shift the Fermi level of the ITO toward the LUMO of PCBM efficiently.

In 2009, Lee et al. reported tandem OPV devices with IZO based intermediate layer [96]. The reason for the author to choose IZO is that it can provide a higher conductivity and transmittance than ITO when deposited at room temperature [97]. The IZO was deposited by facing-

target sputtering technique to minimize the damage effect. In order to avoid $V_{oc}$ reduction by the high work function of the IZO, a very thin layer of LiF, Rubidium carbonate ($Rb_2CO_3$), or $Cs_2CO_3$ was inserted between IZO and the bottom cell. The structure of the tandem device was ITO/PEDOT:PSS (40 nm)/P3HT:PCBM (120 nm)/interlayer/IZO (50 nm)/CuPc (20 nm)/$C_{60}$ (20 nm)/BCP (10 nm)/Al. For comparison, the function of LiF, $Rb_2CO_3$, or $Cs_2CO_3$ interlayer at the IZO cathode was investigated. The 0.5 nm LiF interlayer can not change the IZO layer to become a good cathode and leads to a S-type shaped I–V curve, which is consist with Sakai and Kawano's results [95]. In contrast, the 1 nm alkali carbonate interlayer leads to an ohmic contact at the PCBM/IZO interface. The $V_{oc}$ of the tandem device with alkali carbonate/IZO intermediate layers was 0.96 V, which was close to the sum of the $V_{oc}$ of each single cell. However, in their experiments, the IZO surface was treated by UV ozone for 10 minutes before the deposition of the top cell. The exposure of the device in the UV ozone is harmful to the polymer layer of the bottom cell. In addition, the very thin LiF or alkali carbonate layer cannot protect the bottom active layer from sputter damage. Therefore further improvements can be expected, e.g. by combining it with an inverted solar cell introduced in 2006 [32], since the hole transport layer (transition metal oxide or PEDOT:PSS) thickness can be much thicker without reducing cell efficiency.

### 2.3 Intermediate Layer(s) in Novel Tandem OPV Devices

In the tandem solar cells discussed above, the subcells are electronically coupled in series, such architectures result in an evident dependence of the PCE on the current match of the individual cells. Alternatively, some novel multi-terminal tandem devices were proposed.

In 2007, Hadipour et al. reported a novel polymer tandem solar cell with four terminals, in which the two sub cells are separated by a solution-processed insulating optical spacer with a tunable thickness [98]. The device structure is shown in Figure 18. The main purpose of this work was to decouple the electrical and the optical optimization of the devices and hence obtain tandem devices with improved performance. The thickness of the functional layers in each cell can be optimized for its electrical performance. The two subcells can be connected in series or in parallel, or even working separately, which is beneficial to make good use of the photocurrent from each cell. However, the major problem of achieving this kind of device is still the design and fabrication of the intermediate layer. Unlike the two-terminal devices, in which the electron current and hole current from top and bottom cell only transport several tens of nanometer to neutralize with each other in the intermediate layers, the current in four-terminals tandem device has to transport laterally over a long distance. This requires intermediate layers to have much higher lateral conductivity. As mentioned in Peumans's work [26], a sheet resistance of the intermediate electrode should roughly be less than 25 Ω/square to avoid considerable energy loss. In Hadipour's work, metal electrode like symb (Sm) (3 nm)/Au (12 nm) and Au (20 nm)/PEDOT:PSS (50 nm) was used to ensure the conductivity of the middle electrodes. However the transparency of the intermediate layer is low when the metallic layer is used. As to the electrical connection of the two subcells, the author compared the series connection and parallel connection and found the parallel connection provided a higher output. Interestingly, from Shrotriya's work [99], the PCE of tandem devices with parallel connection is also found to be higher than that of devices with series connection.

In 2010, Sista reported tandem solar cell with a three-terminal structure, where the two subcells were connected in parallel [100]. The three-terminal device is proposed to be relatively simple and straight forward. In this case, the middle electrode was the common anode or cathode for each cell, which means one of the subcells should be an inverted cell. In the common cathode case, the author used $TiO_x$:Cs/Al (3 nm)/Au (12 nm)/ $TiO_x$:Cs as the intermediate cathode. The ultra-thin Al layer was used to prevent the penetration and diffusion of Au atoms into the bottom cell. The UPS results show that the work function of Au layer was shifted to 3.5 eV by the $TiO_x$:Cs layer. In the common anode, PEDOT:PSS/Au (12 nm)/$V_2O_5$ was used as the intermediate anode. Due to the fact that direct contact between Au and organic layers often leads to a surface dipole layer and results in an increased barrier [41, 101], a high work function $V_2O_5$ layer was used to modify the Au surface. The active layer of the subcells were P3HT:$PC_{70}$BM layer and a PSBTBT:$PC_{70}$BM layer: see Figure 19. The common-anode architecture exhibited higher performance,

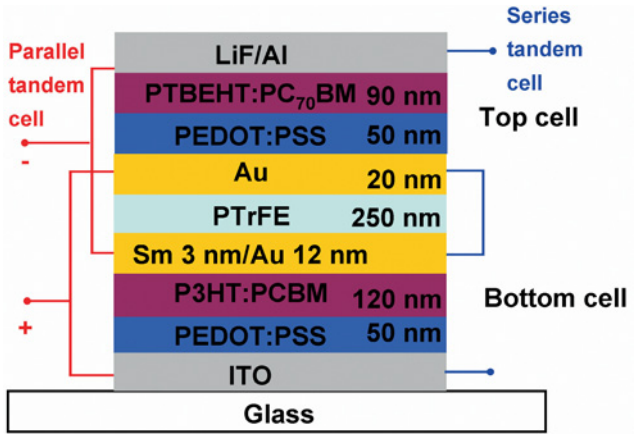


**Figure 18.** Schematic structure of four terminals tandem organic solar cell demonstrated by Hadipour et al. [98], where the two subcells can be connected either in series or in parallel.

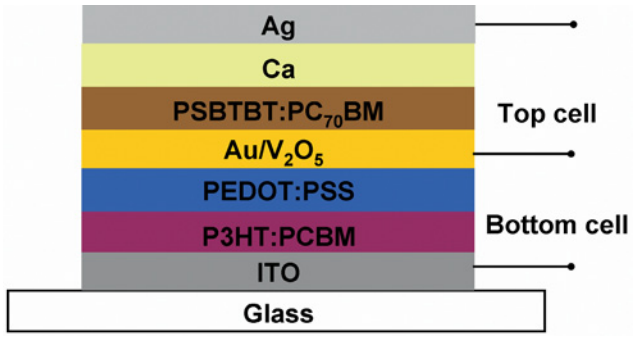


**Figure 19.** Schematic structure of three terminals tandem organic solar cell demonstrated by Sista et al. [100], where the two subcells were connected in parallel, the PEDOT/Au/$V_2$ $O_5$ or $TiO_2$:Cs/Al /Au/ $TiO_2$:Cs were used as common anode or cathode.

with a $V_{oc}$ of 0.60 V, a $J_{sc}$ of 15.1 mA/cm$^2$, a FF of 52%, and a PCE of 4.8%. Here the $J_{sc}$ is the sum of the $J_{sc}$ of each cell (10.1 mA/cm$^2$ and 5.2 mA/cm$^2$, respectively). Interestingly, the author found that, in the parallel case, the FF of the tandem device is mainly depended on the FF of the subcell with larger photocurrent. This characteristic is much different from that of a "series tandem" device, in which the FF was proven to be mainly determined by the device with lower photocurrent [102, 103]. This provides a different approach in the optimizing of the tandem device.

In 2009, Tanaka et al. demonstrated tandem solar cells with multi-wall carbon nanotube (MWCNT) as the common anode [104]. The device structure is shown in Figure 20. MWCNT have attracted lot of attention due to their high conductivity, high transparence and excellent mechanical properties. The work function of MWCNT is around 5.2 eV, which makes it suitable to be an anode. In their work, the sheet resistance of the MWCNT sheet was around

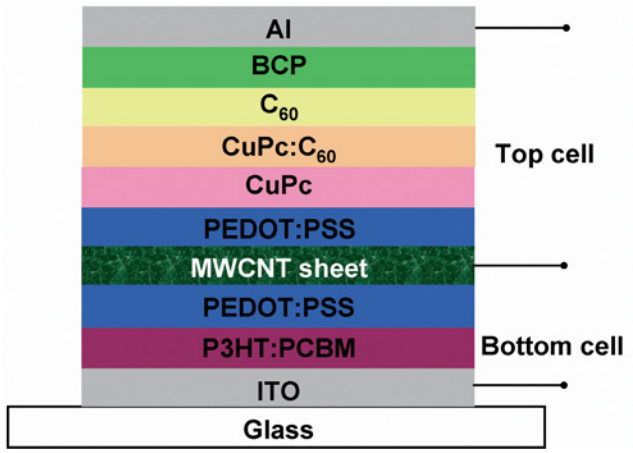


**Figure 20.** Schematic structure of three terminals tandem organic solar cell with MWCNT as intermediate layer demonstrated by Tanaka et al. [104].

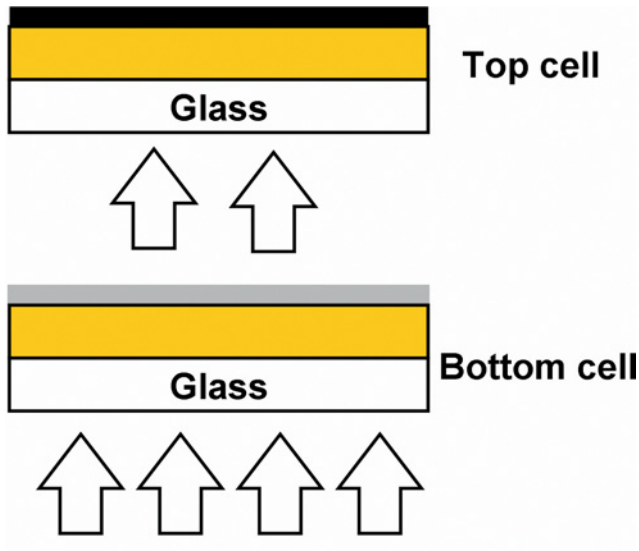


**Figure 21.** Schematic structure of tandem organic solar cells consisted of vertically stacked semitransparent solar cells demonstrated by Shrotriya et al. [99].

500–700 Ω/square, and the transparency of the MWCNT sheet was >85% for perpendicular polarization, >65% for parallel polarization. The MWCNT was grown by chemical vapor deposition to form oriented MWCNT forest. The 20 μm thick MWCNT sheet was transferred to the top of the bottom cell by dry drawn and then densified into a 50–100 nm sheet. The MWCNT sheet was sandwiched by two PEDOT:PSS layers to form the intermediate anode. The PEDOT:PSS was used to platen the MWCNT sheet and to increase the effective contact area. However, the $J_{sc}$ of the tandem device (2.6 mA/cm$^2$) was close to that of single cells (2.3 mA/cm$^2$); The PCE of tandem device (0.31%) was comparable with single cell (0.3%). The FF of the tandem cell and single cell was less than 30%. The low performance was mainly attributed to the bad physics contact between MWCNT sheet and organic layers. Also, the resistance of the MWCNT sheet should be further reduced since the current passing through it is the sum of that in ITO and metal electrodes.

As discussed above, the main merits of employing tandem architecture are: (a) enhancing the light harvesting by the multiple junction architecture; (b) breaking the 10% PCE limit of OPV by combining photoactive materials with different band gaps to make full use of the photon energy [33]. Vertically stacking semitransparent solar cells together can also provides an enhanced light harvesting and higher efficiency up-limit. Shrotriya et al. reported a stacking device with improved light harvesting [99], where the two cells were fabricated on different substrates and one of them was capped by a semitransparent cathode, as show in Figure 21. The $J_{sc}$ or $V_{oc}$ can be summed depending on the connection configuration. In this study, the cells con-

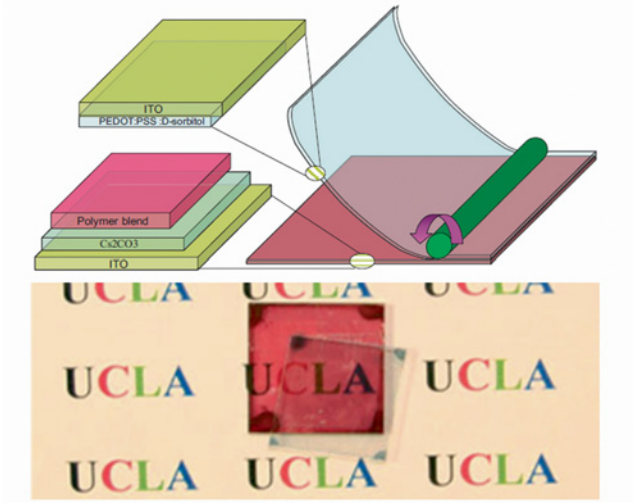


**Figure 22.** Scheme for the lamination method to fabricated semitransparent solar cell and photograph of laminated semitransparent device demonstrated by Huang et al. [105].

nected in parallel show a slightly higher PCE than cells connected in series (2.5% versus 2.4%). The performance of this tandem solar cell is mainly determined by the transmittance of the semitransparent electrode, which needs to be thick enough as charge collecting electrode. In Shrotriya's work, several kinds of metallic multi-layers were compared as the semitransparent cathode. LiF (1 nm)/Al (2.5 nm)/Au (12.5 nm) semitransparent cathode shows the highest transmittance of 75% at the peak absorption wavelength of the active layer (MEH-PPV:PCBM).

The transparence of the "bottom cell" can be further improved by using ITO or IZO layers, which shows the best transparency among the electrodes. However, conventional sputtering processes of ITO or IZO unavoidably cause damage to the active layer. A promising lamination method to fabricated semitransparent solar cell with highly transparent ITO as both anode and cathode was demonstrated [105], as illustrated in Figure 22. The devices with P3HT:PCBM active layer show comparable performance (around 3%) with conventional solar cells with a reflective cathode. This method has the advantage of being low cost and providing high transparency for vertically stacked solar cell applications.

Transparent polymer solar cells are emerging as a promising technology for tandem solar cell application to increase energy conversion efficiency. The transparent polymer solar cells have been reviewed recently [43].

## 3 Conclusion

In organic tandem solar cells, the design of intermediate layers plays a very important role to achieve a high performance device. For conventional tandem devices with subcells connected in series, the intermediate layers should enable efficient charge recombination to prevent the subcells from charging. Ohmic contact between the intermediate layers and the photoactive layers is required to minimize the energy loss when charges entering the intermediate layers from photoactive layers. Otherwise, the total $V_{oc}$ is generally less than the sum of the $V_{oc}$ of each subcell. In addition, a high transparency intermediate layer is always desired. The current balance of the subcells is also of most important factor to be considered in the designing of efficient tandem cell. In tandem devices with unbalanced current from subcells, the high current cell would be consumed to charge the low current subcell, and hence reduce the overall photocurrent of tandem devices. In solution processed tandem OPV devices, the intermediate layers should be able to suffer from subsequent solution process and protect the bottom cells. Despite of all these constrain, several categories of intermediate layers have been successfully demonstrated and studied in the last two decades. Efficient tandem solar cells with a PCE of 5–8% have been achieved in the last few years. In the past few years, there has been a significant progress in the design and synthesis of new low bandgap polymers which produces quiet efficient single layer devices. The combined fast progress of both organic active materials [6–11] and the device engineering like tandem architecture will eventually define the success of the OPV technology.

## References

[1] BP Statistical Review of World Energy 2009, `http://www.bp.com/statisticalreview`.

[2] J. A. Turner, Science 285 (1999), 687–689.

[3] K. M. Coakley and M. D. McGehee, Chem. Mater. 16 (2004), 4533–4542.

[4] G. Li, V. Shrotriya, Y. Yao and J. Huang, J. Mater. Chem. 17 (2007), 3126–3140.

[5] C. J. Brabec, V. Dyakonov and U. Scherf, *A book, Organic Photovoltaics: Materials, Device Physics, and Manufacturing Technologies*. Wiley-VCH: Weinheim, Germany, 2008.

[6] H. Y. Chen, J. Hou, S. Zhang, Y. Liang, G. Yang, Y. Yang, L. Yu, Y. Wu and G. Li, Nat. Photonics 3 (2009), 649–653.

[7] Y. Liang, Z. Xu, J. Xia, S. T. Tsai, Y. Wu, G. Li, C. Ray and L. Yu, Adv. Mater. 22 (2010), E135-E138.

[8] S. H. Park, A. Roy, S. Beaupr, S. Cho, N. Coates, J. S. Moon, D. Moses, M. Leclerc, K. Lee and A. J. Heeger, Nat. Photonics 3 (2009), 297–302.

[9] Y. Liang, Y. Wu, D. Feng, S. T. Tsai, H. J. Son, G. Li and L. Yu, J. Am. Chem. Soc. 131 (2009), 56–57.

[10] G. F. Chen and F. Williams, J. Am. Chem. Soc. 113 (1991), 7792–7794.

[11] J. Hou, H. Y. Chen, S. Zhang, R. I. Chen, Y. Yang, Y. Wu and G. Li, J. Am. Chem. Soc. 131 (2009), 15586–15587.

[12] Online news of Heliatek GmbH, (2010), http://www.heliatek.com/uploads/19-_en.pdf.

[13] C. W. Tang, Appl. Phys. Lett. 48 (1986), 183–185.

[14] M. Hiramoto, H. Fujiwara and M. Yokoyama, J. Appl. Phys. 72 (1992), 3781–3787.

[15] M. Hiramoto, H. Fujiwara and M. Yokoyama, Appl. Phys. Lett. 58 (1991), 1062–1064.

[16] S. Morita, A. A. Zakhidov and K. Yoshino, Solid State Commun. 82 (1992), 249–252.

[17] K. Yoshino, S. Morita and T. Kawai, Chem. Express 7 (1992), 817–817.

[18] K. Yoshino, X. H. Yin, S. Morita, T. Kawai and A. A. Zakhidov, Solid State Commun. 85 (1993), 85–88.

[19] N. S. Sariciftci, L. Smilowitz, A. J. Heeger and F. Wudl, Science 258 (1992), 1474–1476.

[20] R. D. McCullough, S. Tristram-Nagle, S. P. Williams, R. D. Lowe and M. Jayaraman, J. Am. Chem. Soc. 115 (1993), 4910–4911.

[21] T. A. Chen and R. D. Rieke, J. Am. Chem. Soc. 114 (1992), 10087–10088.

[22] T. A. Chen, X. Wu and R. D. Rieke, J. Am. Chem. Soc. 117 (1995), 233–244.

[23] J. C. Hummelen, G. Yu, J. Gao, F. Wudl and A. J. Heeger, Science 270 (1995), 1789–1791.

[24] J. J. M. Halls, C. A. Walsh, N. C. Greenham, E. A. Marseglia, R. H. Friend, S. C. Moratti and A. B. Holmes, 376 (1995), 498–500.

[25] J. C. Hummelen, B. W. Knight, F. LePeq, F. Wudl, J. Yao and C. L. Wilkins, J. Org. Chem. 60 (1995), 532–538.

[26] P. Peumans, A. Yakimov and S. R. Forrest, J. Appl. Phys. 93 (2003), 3693–3723.

[27] S. E. Shaheen, C. J. Brabec, N. S. Sariciftci, F. Padinger, T. Fromherz and J. C. Hummelen, Appl. Phys. Lett. 78 (2001), 841–843.

[28] G. Li, V. Shrotriya, J. Huang, Y. Yao, T. Moriarty, K. Emery and Y. Yang, Nat. Mater. 4 (2005), 864–868.

[29] L. Li, G. Lu and X. Yang, Polymer 17 (2008), 1984–1990.

[30] X. Yang, J. K. J. van Duren, R. A. J. Janssen, M. A. J. Michels and J. Loos, Macromolecules 37 (2004), 2151–2158.

[31] C. W. Chu, H. Yang, W. J. Hou, J. Huang, G. Li and Y. Yang, Appl. Phys. Lett. 92 (2008), 103306.

[32] G. Li, C. W. Chu, V. Shrotriya, J. Huang and Y. Yang, Appl. Phys. Lett. 88 (2006), 253503.

[33] G. Dennler, M. C. Scharber and C. J. Brabec, Adv. Mater. 21 (2009), 1323–1338.

[34] M. Hiramoto, M. Suezaki and M. Yokoyama, Chem. Lett.1990), 327–330.

[35] A. Yakimov and S. R. Forrest, Appl. Phys. Lett. 80 (2002), 1667.

[36] B. P. Rand, P. Peumans and S. R. Forrest, J. Appl. Phys. 96 (2004), 7519–7526.

[37] J. G. Xue, S. Uchida, B. P. Rand and S. R. Forrest, Appl. Phys. Lett. 85 (2004), 5757–5759.

[38] G. Dennler, H. J. Prall, R. Koeppe, M. Egginger, R. Autengruber and N. S. Sariciftci, Appl. Phys. Lett. 89 (2006), 073502.

[39] I. G. Hill, A. Rajagopal, A. Kahn and Y. Hu, Appl. Phys. Lett. 73 (1998), 662.

[40] K. Seki, N. Hayashi, H. Oji, E. Ito, Y. Ouchi and H. Ishii, Thin Solid Films 393 (2001), 298–303.

[41] L. S. Hung and C. H. Chen, Mater. Sci. & Eng. R 39 (2002), 143–222.

[42] A. G. F. Janssen, T. Riedl, S. Hamwi, H. H. Johannes and W. Kowalsky, Appl. Phys. Lett. 91 (2007), 073519.

[43] J. Huang, G. Li, J.-H. Li, L.-M. Chen and Y. Yang, A section of a book, *Transparent Electronics*, A. Facchetti and T. J. Marks, pp. 343–373, John Wiley & Sons Ltd, 2010.

[44] X. Zhou, M. Pfeiffer, J. Blochwitz, A. Werner, A. Nollau, T. Fritz and K. Leo, Appl. Phys. Lett. 78 (2001), 410–412.

[45] K. Walzer, B. Maennig, M. Pfeiffer and K. Leo, Chem. Rev. 107 (2007), 1233–1271.

[46] B. Maennig, J. Drechsel, D. Gebeyehu, P. Simon, F. Kozlowski, A. Werner, F. Li, S. Grundmann, S. Sonntag, M. Koch, K. Leo, M. Pfeiffer, H. Hoppe, D. Meissner, N. S. Sariciftci, I. Riedel, V. Dyakonov and J. Parisi, Appl. Phys. A-Mater. 79 (2004), 1–14.

[47] J. Drechsel, B. Mannig, F. Kozlowski, M. Pfeiffer, K. Leo and H. Hoppe, Appl. Phys. Lett. 86 (2005), 244102.

[48] A. Colsmann, J. Junge, C. Kayser and U. Lemmer, Appl. Phys. Lett. 89 (2006), 203506.

[49] R. Schueppel, R. Timmreck, N. Allinger, T. Mueller, M. Furno, C. Uhrich, K. Leo and M. Riede, J. Appl. Phys. 107 (2010), 044503.

[50] B. Yu, F. Zhu, H. B. Wang, G. Li and D. H. Yan, J. Appl. Phys. 104 (2008), 114503.

[51] L. S. Hung, C. W. Tang and M. G. Mason, Appl. Phys. Lett. 70 (1997), 152–154.

[52] H. Fujikawa, T. Mori, K. Noda, M. Ishii, S. Tokito and Y. Taga, J. Lumin. 87:9 (2000), 1177–1179.

[53] P. Piromreun, H. Oh, Y. L. Shen, G. G. Malliaras, J. C. Scott and P. J. Brock, Appl. Phys. Lett. 77 (2000), 2403–2405.

[54] T. R. Briere and A. H. Sommer, J. Appl. Phys. 48 (1977), 3547.

[55] C. I. Wu, C. T. Lin, Y. H. Chen, M. H. Chen, Y. J. Lu and C. C. Wu, Appl. Phys. Lett. 88 (2006), 152104.

[56] J. S. Huang, Z. Xu and Y. Yang, Adv. Funct. Mater. 17 (2007), 1966–1973.

[57] J. S. Huang, G. Li and Y. Yang, Adv. Mater. 20 (2008), 415–419.

[58] J. Huang, G. Li, E. Wu, Q. Xu and Y. Yang, Adv. Mater. 18 (2006), 114–117.

[59] J. Huang, T. Watanabe, K. Ueno and Y. Yang, Adv. Mater. 19 (2007), 739–743.

[60] G. S. Nadkarni and J. G. Simmons, J. Appl. Phys. 41 (1970), 545.

[61] C. W. Chu, S. H. Li, C. W. Chen, V. Shrotriya and Y. Yang, Appl. Phys. Lett. 87 (2005), 193508.

[62] C. Tao, S. P. Ruan, X. D. Zhang, G. H. Xie, L. Shen, X. Z. Kong, W. Dong, C. X. Liu and W. Y. Chen, Appl. Phys. Lett. 93 (2008), 193307.

[63] V. Shrotriya, G. Li, Y. Yao, C. W. Chu and Y. Yang, Appl. Phys. Lett. 88 (2006), 073508.

[64] J. Meyer, S. Hamwi, T. Bulow, H. H. Johannes, T. Riedl and W. Kowalsky, Appl. Phys. Lett. 91 (2007), 113506.

[65] X. L. Zhu, J. X. Sun, H. J. Peng, Z. G. Meng, M. Wong and H. S. Kwok, Appl. Phys. Lett. 87 (2005), 153508.

[66] T. Tsutsui and M. Terai, Appl. Phys. Lett. 84 (2004), 440–442.

[67] C. C. Chang, J. F. Chen, S. W. Hwang and C. H. Chen, Appl. Phys. Lett. 87 (2005), 253501.

[68] C. W. Chen, Y. J. Lu, C. C. Wu, E. H. E. Wu, C. W. Chu and Y. Yang, Appl. Phys. Lett. 87 (2005), 241121.

[69] D. W. Zhao, X. W. Sun, C. Y. Jiang, A. K. K. Kyaw, G. Q. Lo and D. L. Kwong, Appl. Phys. Lett. 93 (2008), 083305.

[70] J. Y. Kim, S. H. Kim, H. H. Lee, K. Lee, W. L. Ma, X. Gong and A. J. Heeger, Adv. Mater. 18 (2006), 572–576.

[71] F. C. Chen and C. H. Lin, J. Phys. D: Appl. Phys. 43 (2010), 025104.

[72] T. Mori, H. Fujikawa, S. Tokito and Y. Taga, Appl. Phys. Lett. 73 (1998), 2763–2765.

[73] M. G. Mason, C. W. Tang, L. S. Hung, P. Raychaudhuri, J. Madathil, D. J. Giesen, L. Yan, Q. T. Le, Y. Gao, S. T. Lee, L. S. Liao, L. F. Cheng, W. R. Salaneck, D. A. dos Santos and J. L. Bredas, J. Appl. Phys. 89 (2001), 2756–2765.

[74] A. Hadipour, B. de Boer, J. Wildeman, F. B. Kooistra, J. C. Hummelen, M. G. R. Turbiez, M. M. Wienk, R. A. J. Janssen and P. W. M. Blom, Adv. Funct. Mater. 16 (2006), 1897–1903.

[75] D. W. Zhao, X. W. Sun, G. Q. Lo and D. L. Kwong, IEEE Electron Device Lett. 30 (2009), 490.

[76] J. Gilot, M. M. Wienk and R. A. J. Janssen, Appl. Phys. Lett. 90 (2007), 143512.

[77] A. L. Roest, J. J. Kelly, D. Vanmaekelbergh and E. A. Meulenkamp, Phys. Rev. Lett. 89 (2002), 036801.

[78] W. J. E. Beek, M. M. Wienk, M. Kemerink, X. N. Yang and R. A. J. Janssen, J. Phys. Chem. B 109 (2005), 9505–9516.

[79] J. Gilot, I. Barbu, M. M. Wienk and R. A. J. Janssen, Appl. Phys. Lett. 91 (2007), 102013.

[80] J. Gilot, M. M. Wienk and R. A. J. Janssen, Adv. Mater. 22 (2010), E67-E71.

[81] D. J. D. Moet, P. de Bruyn and P. W. M. Blom, Appl. Phys. Lett. 96 (2010), 153504.

[82] T. W. Lee, O. Kwon, M. G. Kim, S. H. Park, J. Chung, S. Y. Kim, Y. Chung, J. Y. Park, E. Han, D. H. Huh, J. J. Park and L. Pu, Appl. Phys. Lett. 87 (2005), 231106.

[83] J. Y. Kim, K. Lee, N. E. Coates, D. Moses, T. Q. Nguyen, M. Dante and A. J. Heeger, Science 317 (2007), 222–225.

[84] S. Sista, M. H. Park, Z. R. Hong, Y. Wu, J. H. Hou, W. L. Kwan, G. Li and Y. Yang, Adv. Mater. 22 (2010), 380–383.

[85] C. Uhrich, R. Schueppel, A. Petrich, M. Pfeiffer, K. Leo, E. Brier, P. Kilickiran and P. Baeuerle, Adv. Funct. Mater. 17 (2007), 2991–2999.

[86] M. H. Park, J. H. Li, A. Kumar, G. Li and Y. Yang, Adv. Funct. Mater. 19 (2009), 1241–1246.

[87] J. Wang, J. Polleux, J. Lim and B. Dunn, J. Phys. Chem. C 111 (2007), 14925–14931.

[88] J. Kido, T. Nakada, J. Endo, N. Kawamura, K. Mori, A. Yokoi and T. Matsumoto, A paper in proceedings volume, in: Proceedings 11st International Workshop on Inorganic and Organic Electroluminescence and 2002 International Conference on the Science and Technology of Emissive Displays and Lighting, pp. 539 Ghent, Belgium, 2002.

[89] G. Gu, G. Parthasarathy, P. E. Burrows, P. Tian, I. G. Hill, A. Kahn and S. R. Forrest, J. Appl. Phys. 86 (1999), 4067–4075.

[90] D. Vaufrey, M. Ben Khalifa, J. Tardy, C. Ghica, M. G. Blanchin, C. Sandu and J. A. Roger, Semicond. Sci. Technol. 18 (2003), 253–260.

[91] V. Bulovic, P. Tian, P. E. Burrows, M. R. Gokhale, S. R. Forrest and M. E. Thompson, Appl. Phys. Lett. 70 (1997), 2954–2956.

[92] H. K. Kim, K. S. Lee and J. H. Kwon, Appl. Phys. Lett. 88 (2006), 012103.

[93] T. Dobbertin, M. Kroeger, D. Heithecker, D. Schneider, D. Metzdorf, H. Neuner, E. Becker, H. H. Johannes and W. Kowalsky, Appl. Phys. Lett. 82 (2003), 284–286.

[94] K. Kawano, N. Ito, T. Nishimori and J. Sakai, Appl. Phys. Lett. 88 (2006), 073514.

[95] J. Sakai, K. Kawano, T. Yamanari, T. Taima, Y. Yoshida, A. Fujii and M. Ozaki, Sol. Energy Mater. Sol. Cells 94 (2010), 376–380.

[96] B. J. Lee, H. J. Kim, W. I. Jeong and J. J. Kim, Sol. Energy Mater. Sol. Cells 94 (2009), 542–546.

[97] J. W. Kang, W. I. Jeong, J. J. Kim, H. K. Kim, D. G. Kim and G. H. Lee, Electrochem. Solid-State Lett. 10 (2007), J75-J78.

[98] A. Hadipour, B. de Boer and P. W. M. Blom, J. Appl. Phys. 102 (2007), 074506.

[99] V. Shrotriya, E. H. E. Wu, G. Li, Y. Yao and Y. Yang, Appl. Phys. Lett. 88 (2006), 064104.

[100] S. Sista, Z. R. Hong, M. H. Park, Z. Xu and Y. Yang, Adv. Mater. 22 (2010), E77-E80.

[101] N. Koch, J. Phys. Condens. Matter 20 (2008), 184008.

[102] A. Hadipour, B. de Boer and P. W. M. Blom, Org. Electron. 9 (2008), 617–624.

[103] T. Ameri, G. Dennler, C. Lungenschmied and C. J. Brabec, Energy Environ. Sci. 2 (2009), 347–363.

[104] S. Tanaka, K. Mielczarek, R. Ovalle-Robles, B. Wang, D. Hsu and A. A. Zakhidov, Appl. Phys. Lett. 94 (2009), 113506.

[105] J. S. Huang, G. Li and Y. Yang, Adv. Mater. 20 (2008), 415–418.

*Yongbo Yuan received his B.Sc. degree in physics from Sun Yat-sen (Zhongshan) University, China, in 2004 and his Ph.D. degree in condensed matter physics from Sun Yat-sen (Zhongshan) University, China, in 2009. He is currently a Postdoctoral Fellow at University of Nebraska-Lincoln. His research interests include organic optoelectronics, especially solar cells and light emitting devices.*

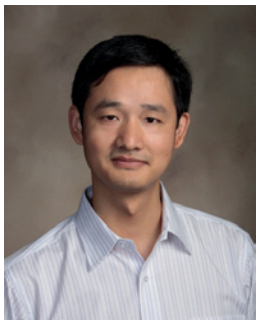

*Jinsong Huang received his PhD degree in Material Science and Engineering from University of California-Los Angeles in 2007. After working in Agiltron Inc as a research scientist for two years, he joined University of Nebraska-Lincoln (UNL) as an assistant professor in the Department of Mechanical Engineering and Nebraska Center for Materials and Nanoscience. His research goals include (i) combining material engineering with interface engineering to boost the performance of organic electronics devices (ii) designing new device architecture and fabrication process to realize low cost and high performance devices and (iii) synthesis high quality nanoparticles and integrate the nanoparticles into organic electronic devices for solid state lighting, energy conversion, energy storage, and low-cost sensor application. He is the recipient of multiple awards including DTRA Young Investor Award in 2010, Materials Research Society Graduate Student Awards (2006), Chinese Government Award for Outstanding Self-finance Students Abroad (2006).*

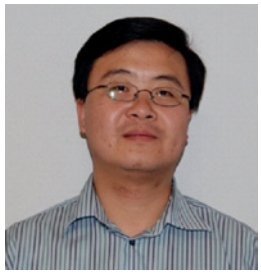

*Gang Li's Bachelor's degree is from Wuhan University. He received his MS degree in EE and PhD degree in Condensed Matter Physics in 2003, both from Iowa State University, where his research focused on organic light emitting devices (OLEDs). From 2004 to 2007, he conducted postdoctoral research in Prof. Yang Yang's group in the Dept. of Materials Science and Engineering (MSE) at UCLA, focusing on polymer solar cells and also on polymer light emitting devices (PLEDs). He has published over 40 scientific articles in academic journals such as Nature Materials, Nature Photonics, Advanced Materials, JACS, Physics Review B etc. and 3 book chapters. He also filed multiple patent applications in the area of organic electronics. Dr. Li has been with Solarmer Energy Inc. since June 2007, and is now the VP of Engineering.*